Foundations of Physics, Vol. 31, No. 2, 2001

Test of Trace Formulas for Spectra of Superconducting Microwave Billiards[1]

A. Richter[2]

Received August 15, 2000

Experimental tests of various trace formulas, which in general relate the density of states for a given quantum mechanical system to the properties of the periodic orbits of its classical counterpart, for spectra of superconducting microwave billiards of varying chaoticity are reviewed by way of examples. For a two-dimensional Bunimovich stadium billiard the application of Gutzwiller's trace formula is shown to yield correctly locations and strengths of the peaks in the Fourier transformed quantum spectrum in terms of the shortest unstable classical periodic orbits. Furthermore, in two-dimensional billiards of the Limaçon family the transition from regular to chaotic dynamics is studied in terms of a recently derived general trace formula by Ullmo, Grinberg and Tomsovic. Finally, some salient features of wave dynamical chaos in a fully chaotic three-dimensional Sinai microwave billiard are discussed. Here the reconstruction of the spectrum is not as straightforward as in the two-dimensional cases and a modified trace formula as suggested by Balian and Duplantier will have eventually to be applied.

1. INTRODUCTION

Quantum manifestations of classical chaos have received much attention in recent years.(1) The spectral fluctuation properties of systems which are fully chaotic in the classical limit were investigated both analytically and numerically. Generically, it has been found that these properties coincide with those of the ensembles from Random Matrix Theory (RMT) having the proper symmetry.(2, 3) For time-reversal invariant systems, the relevant ensemble is the Gaussian orthogonal ensemble (GOE), for a recent review of RMT in quantum physics see Ref. 4.

[1] This paper is dedicated to Martin Gutzwiller on the occasion of his 75th birthday. Work supported by the Deutsche Forschungsgemeinschaft under contract No. RI 242/16-1.

[2] Institut für Kernphysik, Technische Universität Darmstadt, D-64289 Darmstadt, Germany.

0015-9018/01/0200-0327$19.50/0

Due to the pioneering work of Martin Gutzwiller[5] the semiclassical relationship between the density of states of a chaotic quantum system and the properties of the periodic orbits (POs) of the corresponding classical system is known for nearly 30 years.[5] The so-called Gutzwiller trace formula expresses the density of states by a weighted sum over all individual classical POs. Integrable, i.e., regular, systems can be described by Einstein–Brillouin–Keller (EBK) quantization.[6] A trace formula for such systems was also first derived by Gutzwiller[7] and later in a different way by Berry and Tabor.[8] Beside these two limiting cases of chaotic and regular dynamics respectively, systems with intermediate, mixed behavior have attracted more and more attention recently.[9]

In the last few decades the theoretical investigation of two-dimensional Euclidian and Riemannian geometries, so-called billiards, has led to a very fruitful new discipline in non-linear physics.[10–13] Due to the conserved energy of the ideal particle propagating inside the billiard's boundaries with specular reflections on the walls, the plain billiard belongs to the class of Hamiltonian systems with the lowest degree of freedom in which chaos can occur and this does only depend on the given boundary shape. Because of their simplicity two-dimensional billiards are in particular useful for studying the behavior of the particle in the corresponding quantum regime[3, 14, 15] where spectral properties are completely described by the stationary Schrödinger equation

$$H\Psi(\vec{r}) = -\frac{\hbar^2}{2m}\Delta\Psi(\vec{r}) = \mathscr{E}\Psi(\vec{r}) \tag{1}$$

inside the domain $\mathscr{G}$ with Dirichlet boundary conditions on the walls

$$\Psi(\vec{r})|_{\partial\mathscr{G}} = 0 \tag{2}$$

In this context the investigation of "Quantum Chaos" has become one of the most fascinating goals of theoretical physics at the end of this century.[1, 16]

About ten years ago experimentalists have even found very effective techniques to simulate the quantum billiard problem with the help of macroscopic devices. Due to the equivalence of the stationary Schrödinger equation and the classical Helmholtz equation in two dimensions one is able to model the billiard by a similarly shaped electromagnetic cavity.[17–22] Former publications have demonstrated the high accuracy of large ensembles of measured eigenvalues as well as of resonance line shapes and their corresponding widths in two-dimensional *superconducting* cavities formed like desymmetrized Bunimovich stadium and truncated Hyperbola billiards[20, 23–25] and also in coupled Bunimovich stadium billiards.[26]

But also three-dimensional superconducting billiards have been investigated in the past.[27, 28] Due to the polarization properties of the electromagnetic fields $\vec{E}$ and $\vec{B}$ inside the cavity the full vectorial Helmholtz equations[29]

$$\left(\Delta + \varepsilon\mu \frac{\omega^2}{c^2}\right) \vec{E}(\vec{r}) = \vec{0} \tag{3}$$

$$\left(\Delta + \varepsilon\mu \frac{\omega^2}{c^2}\right) \vec{B}(\vec{r}) = \vec{0} \tag{4}$$

have to be used with corresponding boundary conditions

$$\vec{E}_{||}(\vec{r})|_{\partial\mathcal{G}} = \vec{0} \qquad \text{and} \qquad \vec{B}_{\perp}(\vec{r})|_{\partial\mathcal{G}} = \vec{0} \tag{5}$$

on the walls which are assumed to be ideally conducting. Of course the analogy with the corresponding scalar Schrödinger equation in the same geometry is fully lost. Instead of talking of the semiclassical limit one has to describe the classical electromagnetic billiard in this region in terms of ray-optical characteristics, where features of the periodic orbits inside the geometry dominate the corresponding wave optical side.

Three-dimensional systems have so far only scarcely been investigated experimentally. The first experiments with electromagnetic waves in cavities simulating acoustic wave phenomena in rooms were performed by Schröder.[30] Acoustic model statistics in metal blocks have also been investigated.[31, 32] Very recently statistical properties of eigenfrequency distributions in asymmetrically shaped microwave cavities have been reported.[33] Theoretically quantum effects as well as their electromagnetic counterparts in three-dimensional systems were treated in Refs. 34–37.

The present article rests very much upon but updates a previous review.[38] It is organized as follows. In Sec. 2 a description of the experimental methods used to measure the resonance frequencies of the microwave resonators is given. By using a quarter of a Bunimovich stadium billiard, which was measured with highest resolution of all superconducting billiards so far, two approaches towards the description of quantum systems are discussed in Sec. 3. The first approach relies on the analysis of the eigenfrequency spectra with methods of the Random Matrix Theory followed by the comparison with the behavior of the corresponding classical system. The second approach is based on the Periodic Orbit Theory where the knowledge of the properties of the classical periodic orbits enables one to reconstruct the quantum mechanical spectrum. In this context the trace formula of Gutzwiller plays the prime role in the application to the experimental data. In Sec. 4 the semiclassical description of quantum

spectra with trace formulas is extended to near-integrable systems. This investigation is performed with billiards of the Limaçon family.[39] The experimental study of spectral properties of a three-dimensional Sinai billiard in Sec. 5 allows to investigate the vectorial Helmholtz equation, i.e., a non-quantum wave equation for classically totally chaotic systems, and to generalize some aspects of quantum chaos. Furthermore, some results on polarization features of electromagnetic waves and important experimental facts in case of three-dimensional cavities are gained. Finally, an outlook is given in Sec. 6.

2. EXPERIMENTAL MATTERS

The electromagnetic cavity is characterized by the stationary Helmholtz equation

$$\Delta \vec{E} = -k^2 \vec{E} \tag{6}$$

with the eigenvalue $k = (2\pi f)/c$, f denoting the frequency (measured in cycles per second, i.e., in Hz) and c stands for the velocity of light, and the electromagnetic field $\vec{E}$ vanishes on the boundary. In case of a sufficiently flat cavity $\vec{E}$ is always perpendicular to the bottom and the top, i.e., one has

$$\vec{E} = |\vec{E}|\, \vec{e}_z \tag{7}$$

In the two-dimensional case the Helmholtz equation is of the form of the stationary Schrödinger equation (1) rewritten as

$$\Delta \Psi(\vec{r}) = -k^2 \Psi(\vec{r}) \tag{8}$$

with the eigenvalue $k = (2m\mathscr{E})^{1/2}/h$, m and $\mathscr{E}$ denoting the mass and the energy of the particle, respectively, and where Ψ vanishes on the boundary.

This means that Eqs. (6) and (8) are identical and have identical eigenvalues and eigenfunctions. Therefore, in a cavity with height $d \leqslant \lambda_{\min}/2 = c/2f_{\max}$ with $\lambda_{\min}$ being the minimum wavelength accessible in the experiments—such a cavity is called two-dimensional—the quantum mechanical motion of a particle in a potential can be simulated with electromagnetic waves.

The solutions of Eq. (6), or equivalently Eq. (8), are discrete eigenvalues k^2 with corresponding eigenfunctions Ψ and $\vec{E}$, respectively. The

chaotic behavior of billiards is thus characterized by the distribution of those quantities.

For a precise test of the spectra of eigenmodes in terms of the various statistical measures as discussed further on, a highly accurate measurement of the resonances, i.e., their locations and widths, is necessary. Therefore superconducting niobium cavities built in the CERN workshops at Geneva are used, yielding quality factors $Q = f/\Delta f \approx 10^5$ to 10^7 compared with a Q of about 10^3 for normal conducting cavities.[38] The first measurements were done in the cryostats of the superconducting Darmstadt electron linear accelerator S-DALINAC,[40] but soon the construction of a new LHe bath cryostat became necessary. This cryostat, dedicated to experiments on chaos, offers on the one hand very stable measurement conditions (no disturbance of pressure fluctuations) and on the other hand permanent access to the billiards in contrast to the accelerator, which is opened usually only once or twice a year. Also measurements in which cavity parameters can be varied became possible.[26, 41]

As has been described and shown in Ref. 38 in more detail the cavities are put into a copper box which is completely bathed within the liquid helium, so that the box is at very constant temperature of 4.2 K. The microwave power to excite the cavities is generated by the test set radio-frequency source of an HP-8510B network analyzer and is fed by semi-rigid copper cables into one antenna of the billiard and transmitted by another or reflected by the same antenna. The capacitively coupling dipole antennas sit in small holes on the niobium surface and penetrate only up to a maximum of 0.5 mm into the cavity to keep perturbations of the electromagnetic field inside the resonator as small as possible. In frequency steps as small as 1 Hz over the frequency range $45\ \text{MHz} \leqslant f \leqslant 20\ \text{GHz}$, the analyzer measures the ratio of the outcoming to the ingoing microwave power.

In Fig. 1 a small sequence of the eigenmode spectrum of a Limaçon billiard discussed in Sec. 4 is plotted. One sees the very sharp resonances in the lower part of the figure where the billiard is superconducting, distinctly different with respect to the wider resonances in the normal conducting case in the upper part of the picture. The width reduction of the resonances by a factor of about 1000 in the superconducting case allows to resolve even very close resonances ($\Delta f < 100\ \text{kHz}$) compared to the mean level spacing of about several MHz in this part of the spectrum. The closest resonances observed have a spacing of about 300 MHz so that we are sure not have missed modes by overlapping spacings. On the other hand there is the possibility that one might miss modes which have nearly no electromagnetic field at the position of the antennas. To reduce this possibility, measurements are always made with differently placed antennas. Thereby, the number of missed modes is dramatically reduced below three to five in

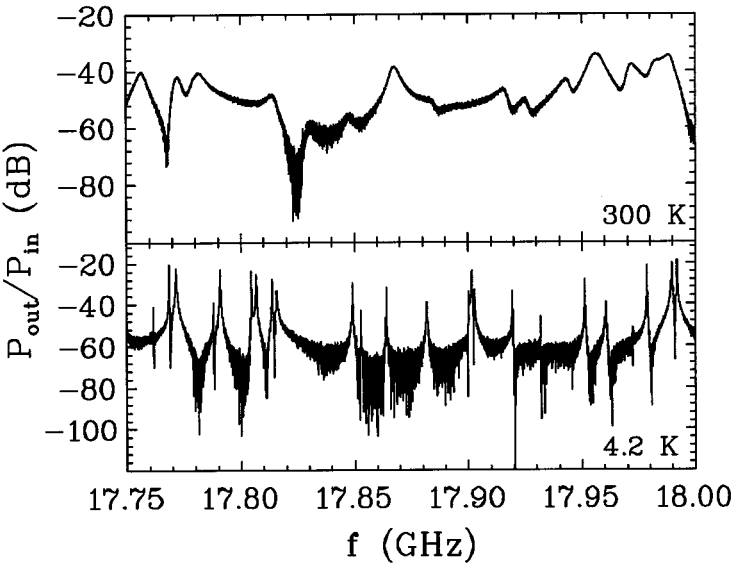

Fig. 1. Small sequence of the eigenmode spectrum of a Limaçon billiard (see Sec. 4) in the frequency range 17.75 GHz $\leqslant f \leqslant$ 18.00 GHz, where the density of eigenmodes is already very high. In the upper half a spectrum of a Niobium cavity taken at room temperature is shown, in the lower part a spectrum at 4.2 K, where the billiard cavity is superconducting. Note the excellent resolution of the spectrum at low temperature as compared to the one at room temperature and the frequency shift of the eigenmodes due to the contraction of the cavity at 4.2 K.

a typical case of a measurement of one thousand eigenmodes as can, e.g., be estimated from the area and the perimeter with the help of the Weyl formula (see Sec. 3).

Here a general remark is in order. Often the statement is made, that the eigenmode spectrum of any billiard (of a not too extraordinary shape) —a so-called *ideal* billiard—can nowadays with modern computers be simulated with high precision, i.e., with a very small uncertainty in the position of a given eigenvalue. To the contrary in the experiment always a *real* billiard is studied which naturally might have smaller or larger mechanical imperfections, shrinks in size when cooled down to low temperatures and is excited by antennas reaching into the volume of the resonator. This explains why there might be slight shifts between simulated and measured eigenvalues for any given billiard. They are, however, generally understood as has been shown for several of the billiards discussed here[23, 42] and it can be stated firmly, that the high quality factor Q up to about 10^7 obtained in our superconducting billiards is sufficient to

resolve all eigenmodes up to a frequency of 20 GHz and even higher. The typical area of the two-dimensional billiards is $A \approx 10^3$ cm^2, which results in about 10^3 eigenmodes. Furthermore, an example for a detailed comparison of a length spectrum of periodic orbits in a *real* Bunimovich stadium deduced from measurements of eigenmodes and of a corresponding computed one from an *ideal* stadium will be presented at the end of the next section.

3. FIRST EXAMPLE: THE BUNIMOVICH STADIUM BILLIARD

In this section results are discussed—reported in detail in Ref. 20—obtained with a superconducting niobium cavity, which has the shape of a quarter Bunimovich stadium billiard with inner dimensions $r = 200$ mm (radius of the quarter circle), $a = 360$ mm (length of the straight part of the rectangle) and height $d = 8$ mm corresponding to $\gamma = a/r = 1.8$ (see Fig. 2) at room temperature. The relative uncertainties in those dimensional measures of the cavities due to their fabrication are less than 1 percent. With only a quarter of a stadium, one is restricted to a single symmetry class of the full problem.[43] As indicated in Fig. 2, three antennas were located in small holes (4 mm diameter). To keep their influence on the field

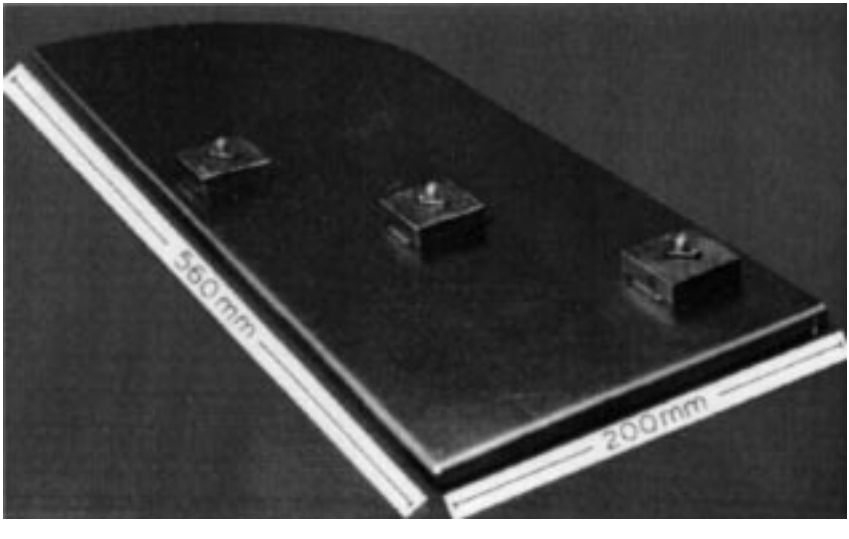

Fig. 2. Flat niobium resonator with the shape of a quarter of a Bunimovich stadium. Three input microwave connectors feeding the antennas are mounted on the top of the billiard (from Ref. 38).

distributions negligibly small but guaranteeing at same time signals of a detectable level they were adjusted to penetrate less than 500 μm into the cavity. To ensure the two-dimensionality of the cavity the analysis of the spectra has been confined to $f < 17.5$ GHz. Up to this frequency 1060 eigenmodes were counted.

The three major steps in the analysis of the data according to the methods of RMT are described in the following: From the eigenvalue sequence ("stick" spectrum) a level density $\rho(f) = \sum_i \delta(f - f_i)$ is calculated and a staircase function $N(f) = \int \rho(f')\, df'$ is constructed which fluctuates around a smoothly varying part (defined as the average of $\rho(f)$). The latter usally is related to the volume of the classical energy-allowed phase space, and for billiards an improved version is given by the Weyl formula,[44, 45] which also includes surface corrections

$$N^{\text{Weyl}}(f) = \frac{A\pi}{c^2} f^2 \mp \frac{C}{2c} f + \text{const.} \tag{9}$$

where A is the area of the billiard, C its perimeter and c the velocity of light. The minus and plus signs correspond to Dirichlet and von Neumann boundary conditions, respectively. The remaining fluctuating part of the staircase function $N^{\text{fluc}}(f) = N(f) - N^{\text{Weyl}}(f)$ oscillates around zero. While Eq. (9) does not contain *any* information regarding the character of the underlying classical dynamics of the system, the fluctuating part of the density does. In order to perform a statistical analysis of the given eigenvalue sequence independently from the particular size of the resonator, the measured spectrum has to be first unfolded, i.e., from the measured sequence of eigenfrequencies $\{f_1, f_2, ..., f_i, ...\}$ the spacings $s_i = (f_{i+1} - f_i)/\bar{s}$ between adjacent eigenmodes have been obtained by calculating the local average $\bar{s}$ from Eq. (9).

The proper normalization of the measured 1060 spacings of eigenmodes then yields as a first statistical measure the nearest neighbour spacing distribution (NND) which is given as $P(s)$ in Fig. 3 in form of a histogram. By comparing $P(s)$ to theoretical expressions one notes that it is not Poissonian but rather GOE like and hence characteristic for a chaotic system. However, the agreement of the data with the GOE prediction is far from being perfect. This can be quantified, e.g., in terms of an ansatz by Brody[46] or by a model of Berry and Robnik[47] which interpolate between the two limiting cases of pure Poissonian and pure GOE behavior for a classical regular and a chaotic system, respectively. In the Berry–Robnik model, a mixing parameter q is introduced, which is directly related to the relative chaotic part of the invariant Liouville measure of the underlying classical phase space in which the motion takes place. For $q = 0$ one has a

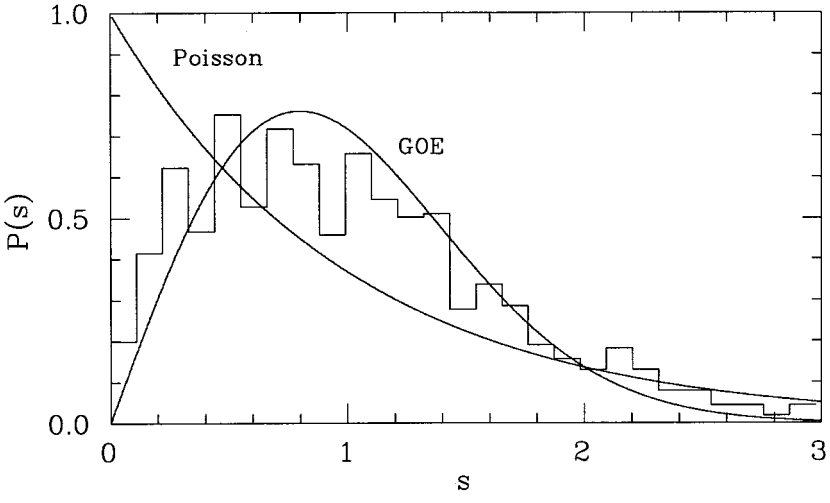

Fig. 3. Nearest neighbour spacing distribution of 1060 eigenvalues measured in the quarter of a superconducting Bunimovich stadium billiard (histogram) compared with a Poisson and GOE distribution, respectively (from Ref. 38).

regular and for $q=1$ a chaotic system. The best fit to the data shown in Fig. 3 yields $q=0.87\pm0.03$. Since the classical stadium is a fully chaotic system this deviation of q from unity is at first surprising.

The reason for this deviation can already be seen, however, in the fluctuating part $N^{\text{fluc}}(f)$ of the integrated eigenvalue density (see the figure displayed over the whole measured frequency range in the upper part of Fig. 4). A strong increase in the amplitude of the fluctuations—a characteristic feature of regular or integrable systems—is observed as well as a periodic gross structure of 750 MHz. This behavior of N^{fluc} is caused by a family of marginally stable periodic orbits, which bounce between the two straight segments of the billiard as indicated in the inset of the upper part of Fig. 4. The presence of these orbits manifests in the spectrum in two different ways: First, there is an approximate quantization rule given by $k_j r = j\pi$. The experimental data agree with this rule astonishingly well. We were able to identify all predicted values $k_j = 2\pi f_j/c$, within a precision of 1/1000, a consequence of the extraordinary resolution of the superconducting measurement. Second, there exists an additional smooth effect in $\rho(f)$ not accounted for by the Weyl formula, which can be seen in Fig. 4. The cumulative level density, $N(f)=\int df'\rho(f')$, shows smooth periodic oscillations (with fixed period $2\pi/r$) around the value given by the Weyl formula. These facts can be understood[48] by the semiclassical analysis of the

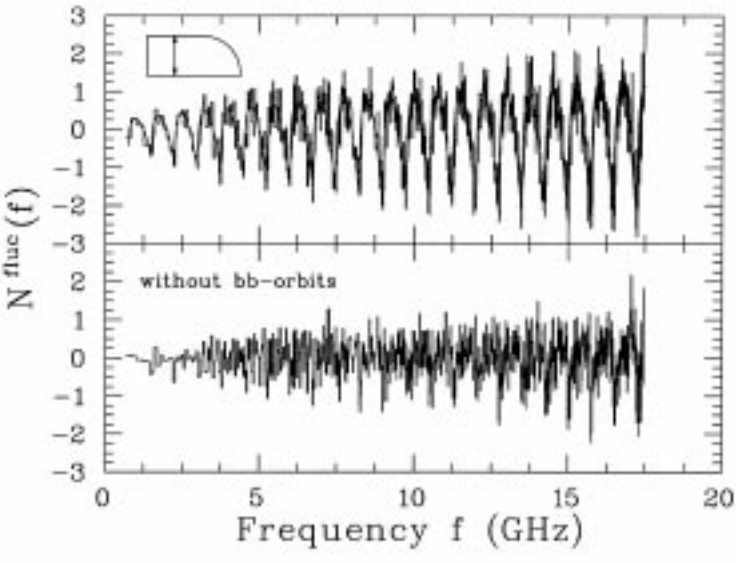

Fig. 4. The histogram in the upper part displays the cumulative level density $N(f)-N^{\mathrm{Weyl}}(f)$. The full line shows the semiclassical prediction of Eq. (10) expressed in terms of the frequency f for the bouncing ball (bb) orbits indicated in the inset. There is excellent agreement between experiment and theory. The lower part expresses $N^{\mathrm{fluc}}(f)$ with the contribution from the bouncing ball orbits substracted (from Ref. 38).

contribution of the bouncing ball orbits to the spectrum, which gives (written in $k=2\pi f/c$ instead of frequency f)

$$N^{\mathrm{BBO}}(k)=\frac{a}{r}\left(\sum_{1\leqslant n\leqslant X}\sqrt{X^2-n^2}-\frac{\pi}{4}X^4+\frac{1}{2}X\right) \tag{10}$$

with $X=kr/\pi$. This formula very nicely reproduces the experimental data as shown in the upper part of Fig. 4. Only after addition of this smooth correction to the Weyl formula is the proper fluctuating part of the level density obtained from the data which is plotted in the lower part of Fig. 4.

Returning to the NND discussed above it can be stated that after the contributions of the bouncing ball orbits are removed from the measured eigenvalue density the experimental result is in perfect agreement with the GOE prediction expressed through a mixing parameter $q=0.97\pm0.02$. Another standard statistical test, the Δ_3 or Dyson–Metha statistics, which measures long-range correlations of eigenvalues in the spectrum (i.e., its "stiffness") shows also the striking effects of the bouncing ball orbits (Fig. 5). Their presence changes the rigidity of the spectrum for large values of the

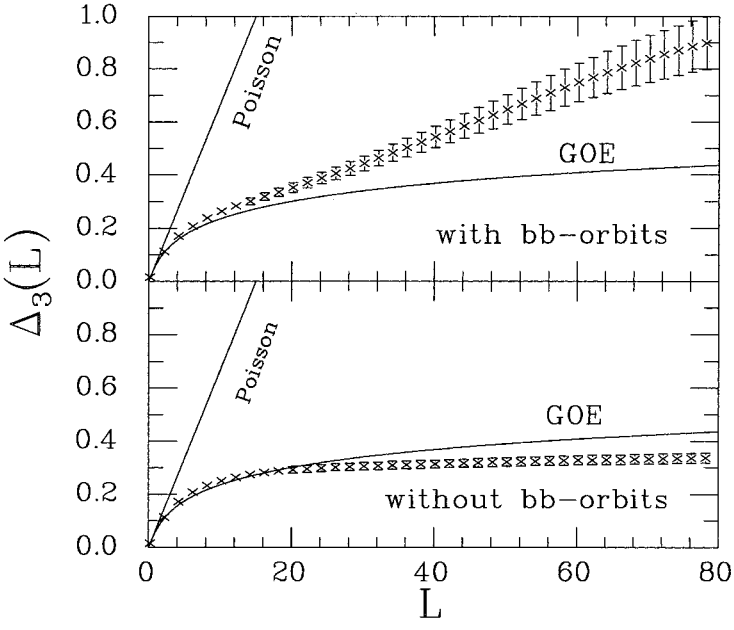

Fig. 5. Upper part: $\Delta_3(L)$ statistics of the experimental data set (crosses with error bars) derived from the unfolded spectrum with the bouncing ball (bb) contributions compared with theoretical predictions. Lower part: without the bouncing ball contributions (from Ref. 38).

length L (measured in terms of the mean level spacing). Proper handling of these orbits—as described above—brings the spectrum near the expected GOE-like behavior of classically chaotic systems. Moreover, the $\Delta_3(L)$ statistics very closely follows the GOE prediction up to $L = 20$, where it saturates, as predicted by Berry.[49] This value of $L = L_{\max}$ defines also the shortest periodic orbit and hence a characteristic time ($L_{\max} \sim 1/\tau_{\min}$), in which the system becomes chaotic.

After the short discussion of the eigenfrequency spectrum of the Bunimovich stadium billiard in terms of the Random Matrix Theory we return now to another important approach towards quantum systems, the Periodic Orbit Theory introduced by Gutzwiller.[1] In general, the chaotic behavior of a classical billiard system expresses itself in the orbits of a point-like particle. If one waits long enough the orbits cover finally the whole phase space. The quantum mechanical analogue, however, does not know orbits anymore but only eigenstates, i.e., wave functions and discrete eigenenergies. The dynamics of the eigenstates then reflects the behavior of the classical orbits.

The semiclassical theory of Gutzwiller assumes that a chaotic system is fully determined through the complete set of its periodic orbits. An orbit is called periodic if a particle after one revolution of length l_μ always returns to the same point in phase space. The effect of the isolated periodic orbits of a billiard is most instructively displayed in the Fourier transformed (FT) spectrum of the eigenvalue density $\rho^{\text{fluc}}(k)$,

$$\tilde{\rho}^{\text{fluc}}(l) = \int_{k_{\min}}^{k_{\max}} dk\, e^{ikl}[\,\rho(k) - \rho^{\text{Weyl}}(k)\,] \tag{11}$$

where $k = 2\pi f/c$, with $[k_{\min}, k_{\max}]$ being the wave number interval in which data were taken. The result of this FT of the measured spectrum of eigenvalues in the quarter of a superconducting Bunimovich stadium billiard is shown in the upper part of Fig. 6. The sharp lines correspond to the lengths l of periodic orbits and the heights of the peaks are a measure for the stability of an orbit. Particularly noticeable is the bouncing ball orbit labeled ① which occurs at $l = 0.4$ m, i.e., twice the width of the billiard, and repeatedly at 0.8, 1.2, 1.6, 2.0,... m. Examples of other prominent periodic orbits that could be identified from the measured spectrum and reconstructed geometrically are also displayed in the figure.

According to the Gutzwiller trace formula,[1, 5] which represents a semi-classical approximation to the quantal density, the fluctuating part of the eigenvalue density is given in terms of the POs, the only elements of the classical dynamics that manifestly survive quantization and are seen in the spectrum.

$$\begin{aligned}\rho^G(S) &= \text{Re} \sum_\mu A(S, \mathbf{M}_\mu) \exp\left(\frac{iS}{\hbar} - i\eta_\mu \frac{\pi}{2}\right) \\ &= \frac{1}{\hbar\pi} \sum_\mu \frac{T_\mu}{|\det(\mathbf{M}_\mu - 1)|^{1/2}} \cos\left(\frac{S}{\hbar} - \eta_\mu \frac{\pi}{2}\right)\end{aligned} \tag{12}$$

Here the index μ labels the periodic orbits and their recurrences, $\mathbf{M}_\mu$ their monodromy matrix, T_μ their period, S their action, which is given for the billiard problem through $\hbar k l_\mu$, and η_μ their Maslov index, where all μ's are isolated. It is Eq. (12) that carries information regarding the chaotic (or regular) character of the classical dynamics and the instability (or stability) of trajectories. This trace formula provides the fundamental relationship between quantum mechanical level density $\rho(S)$ on the left side and the sum over periodic orbits of the corresponding classical system involving their properties on the right hand side.

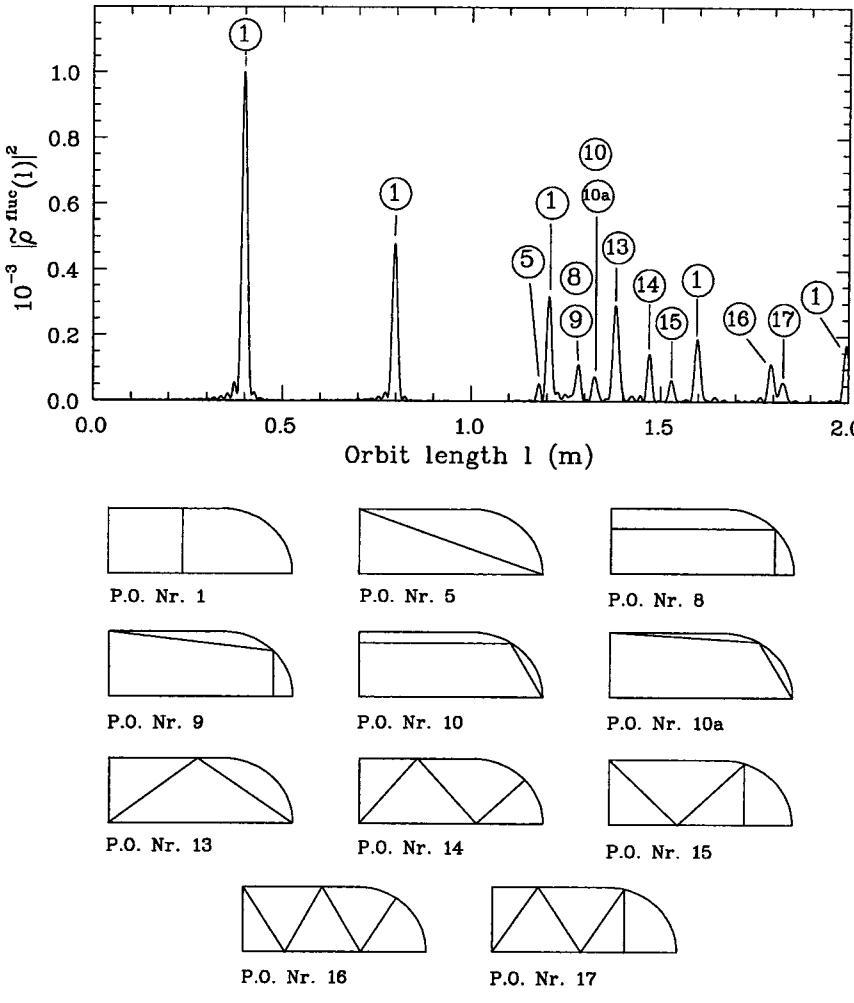

Fig. 6. Fourier transform of the fluctuating part $\rho^{\mathrm{fluc}}(k)$ of the spectrum. The particular orbits labeled with numbers that could be associated with the peaks in the Fourier spectrum up to the length of 2.0 m are also shown (from Ref. 38).

However, the Gutzwiller trace formula is not applicable to all orbits of the stadium billiard. As we know from the discussion above, there is a family of non-isolated marginally stable periodic orbits, that bounce between the two straight segments of the billiard, and those cannot be accounted for by Eq. (12). In Fig. 7 the experimental power spectrum $|\tilde{\rho}^{\mathrm{fluc}}(l)|^2$ of $\rho^{\mathrm{fluc}}(k)$ is compared to the theoretical results (inset) using Eq. (12).

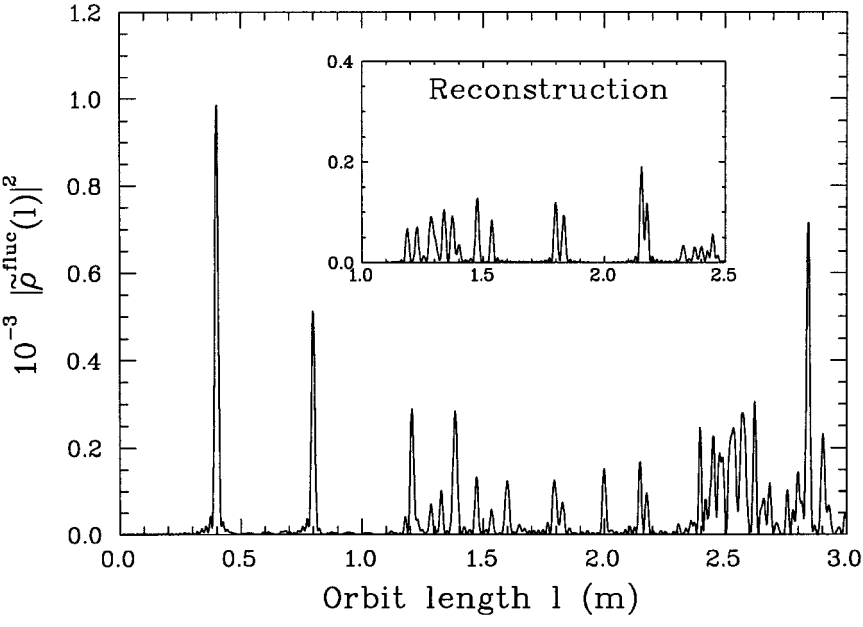

Fig. 7. The same experimental length spectrum as in Fig. 6 but now extending to orbit lengths of 3.0 m compared to a theoretical power spectrum (inset) reconstructed with the help of Gutzwiller's trace formula, Eq. (12) in the main text (from Ref. 38).

The latter has been obtained by identifying the 30 shortest periodic orbits of the system and by calculating their length and monodromy matrix.[50] The monodromy matrix is the matrix which connects a solution of linearized classical equations of motion in the plane perpendicular to the periodic trajectory per period.[43] One is able to reproduce most of the amplitudes up to the length of $l = 2.3$ m, where one starts to miss periodic orbits. For the peak at $l = 1.32$ m corresponding to the so-called "whispering gallery" orbits[43] the contribution of the 10 most stable orbits has been summed. For this family of orbits tr **M** increases fast with the number of collisions with the circular part, so that orbits approaching the circle give a small contribution to the power spectrum. However, one fails to reproduce the amplitude at $l = 1.37$ m, possibly because it is due to a slight geometry imperfection in the experimental set-up at the point where the rectangular part is connected to the half circle.[51] Experimentally a more quantitative statement cannot be made, however, since the microwave cavity is electron beam welded and cannot be opened without destroying it. The two peaks in the theoretical power spectrum correspond to very close trajectories ("whispering gallery-shaped" closed trajectories), they

should be experimentally resolved if the actual shape would exactly coincide with the stadium billiard. For other peaks this small imprecision (if this is the correct explanation) does not imply a sizeable effect. In any case it can be safely stated that the semiclassical analysis is in good agreement with the very precise data measured with high resolution and provides a new scheme for the statistical analysis and comparison with predictions based on the GOE.

At this point it is certainly instructive to return to the point made at the end of Sec. 2, viz. what are the differences in length spectra obtained from a set of measured eigenfrequencies of a superconducting microwave resonator (*real* system) compared to a set calculated numerically (*ideal* system). For this a $\gamma = 1$ Bunimovich stadium has recently been studied.[23] In Fig. 8 the Fourier transform of the fluctuating part $\rho^{\mathrm{fluc}}(k)$ of the eigenvalue density—i.e., the same quantity as in Fig. 6 but with the bouncing ball orbits removed—for the experimental (upper part) and numerical (lower part) data are compared. It can be seen that in addition to the positions of the peaks (length of the POs) also their heights (stability of the POs) are almost identical in the two spectra. Similar conclusions can be drawn from investigations of Ref. 42 for billiards of various shapes also

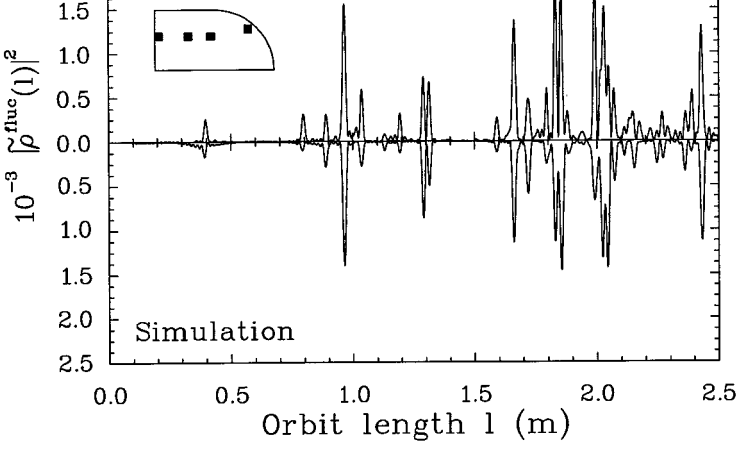

Fig. 8. Fourier transform of the fluctuating part of the level density $\rho(k) - \rho^{\mathrm{Weyl}}(k) - \rho^{\mathrm{BBO}}(k)$ for the $\gamma = 1$ Bunimovich stadium billiard of the shape and with the positions of the antennas shown in the inset. The experimental and numerical results are displayed as mirror images. Remnants of the BBOs at $l = 0.4$ m, 0.8 m, and, to a lesser extent at 1.2 m, are still visible (from Ref. 23).

measured at Darmstadt. So, it is evident from such a comparison that possible small imperfections (like weldseams, antennas, mechanical deformations,...) of the *real* systems have negligible influence on both the statistical analysis (RMT) and the analysis in terms of Periodic Orbit Theory (POT) of the system. To obtain information about two-dimensional billiards, such as presented for the $\gamma = 1.8$ and $\gamma = 1$ stadiums in this section, numerical calculations might have an advantage over measurements, e.g., if one is interested only in eigenvalues. To simulate fairly complex problems numerically such as coupled billiards[26] or the measurement of eigenfunctions[18, 25, 41, 52] is still a different matter. Furthermore, for problems where one is interested in billiards with scatterers inside, billiards with fractal boundaries or three-dimensional billiards, etc., the experiment clearly offers a very convenient way to obtain large sets of eigenvalues quickly.

In summary, the question asked initially in this section, how the behavior of the classical system is transformed into the quantum system, has the following answer for the stadium billiard: There exists a one to one correspondence between the two systems, i.e., after elimination of the (non-generic) bouncing ball orbits in the classical system the analogous quantum mechanical system behaves like the quantal counterpart of a typical chaotic system.

4. SECOND EXAMPLE: THE LIMAÇON BILLIARDS

In this section the semiclassical description of microwave spectra taken from billiards of the Limaçon family will be discussed. The shape of these billiards (also known in mathematics as Pascalian snails) has already been mentioned by the famous German painter Albrecht Dürer in 1525.[53] By varying one control parameter, λ, the system changes from an integrable regular billiard, the circle,[54] through the whole range of billiards with mixed dynamics to a fully chaotic billiard, the cardioid.[55] For a proper description of the billiards with regular and mixed behavior, respectively, another trace formula is necessary, because Gutzwiller's trace formula, discussed in Sec. 3, is only applicable to fully chaotic systems. Such a trace formula for near-integrable systems has recently been derived by Ullmo, Grinberg, and Tomsovic.[9] Their expressions as they remark, however, are being correct to the extent that the Gutzwiller trace formula is valid for large $\Delta S/\hbar$ and will hold even for very large classical perturbations in spite of a derivation whose starting point is first-order classical perturbation theory. As it is shown below in an experimental test using superconducting

billiards of the Limaçon family[39] this trace formula indeed seems to work remarkable well even in case of mixed dynamics.

Before applying the trace formula to the experimental spectra the salient features of it are briefly recalled. One starts with an integrable system, where the contribution of classical periodic orbits with topology $M=(M_1, M_2)$ specifying the individual winding number of the POs on the tori to the density of states is given by the Berry–Tabor formula,[8] which is based on the EBK quantization,

$$\rho_M^{BT}(S)=\frac{T}{\pi h^{3/2} M_2^{3/2} |g_E''|^{1/2}} \cos\left(\frac{S}{h}-\frac{\eta\pi}{2}-\frac{\pi}{4}\right) \tag{13}$$

with T being the period of the periodic orbit, g_E'' the curvature of the line of constant energy $H(I_1, I_2)=E$, S the action of the PO and η its Maslov index.

By moving from the regular into the near-integrable case, Ozorio de Almeida[56] added a small perturbation to an integrable system, which changes the density of states ρ_M^{BT} of the regular system in such a way, that a first order correction to the action has to be added. Introducing a perturbation to a regular system means that the resonant tori, on which the periodic orbits of the regular system exist, are getting destroyed, and only two periodic orbits per torus will survive: one stable (s) and one unstable (u) periodic orbit (according to the Poincaré–Birkhoff theorem). Thus for near-integrable systems Ozorio de Almeida[56] found a modified Berry–Tabor expression for the density of states

$$\rho_M^{O}(S)=\rho_M^{BT} J_0(\Delta S/h) \tag{14}$$

where ΔS is the difference of the action of the stable and unstable orbit, respectively.

In a typical case the unperturbed Hamiltonian and the perturbation of the system are not known. Thus, a generalization of formulae (13) and (14) and also a method to evaluate the parameters entering these formulae is needed.

Ullmo *et al.*[9] started in their evaluation of a trace formula for near-integrable systems also with the Berry–Tabor expression. However, they did not use the propagator formalism of Ref. 8, but instead the energy dependent Green's function and also the result of Ozorio de Almeida. Nevertheless, they went one step further. Instead of truncating the Fourier expansion of the corrected actions, which results in the damping Bessel term in Eq. (14), they mapped the problem onto the pendulum. They introduce an action which is a composition of the mean action $\bar{S}$ and the

difference action ΔS of the two periodic orbits (stable and unstable), $\Delta S = (S_u - S_s)/2$ and $\bar{S} = (S_u + S_s)/2$. The actions S_u and S_s and also the monodromy matrices $\mathbf{M}_u$ and $\mathbf{M}_s$ of the two periodic orbits can be easily computed. Entering these relations into the integral which describes the dephasing of the PO contribution of the family M under a perturbation (see Ref. 9), one is able to modify the expression of the density of states for the integrable case (Berry–Tabor description, Eq. (13)). This yields the following contribution to the density of states for each pair, the stable and the unstable PO,

$$\rho_M^U(S) = \frac{1}{\pi\,|h^3 M_2^3 g_E''|^{1/2}}\ \mathrm{Re}\left\{\exp\left(\frac{i\bar{S}}{h} - \frac{i\eta\pi}{2} - \frac{i\pi}{4}\right) \times\left[\bar{T}[J_0(s) - i\tilde{a}J_1(s)] + i\,\Delta T\left[J_1(s) + \frac{i\tilde{a}}{2}[J_0(s) - J_2(s)]\right]\right]\right\} \tag{15}$$

with $s = \Delta S/h$ being the normalized correction to the action, $\bar{T}$ the averaged period (half of the sum of two periods) and ΔT their difference. The quantities $J_0(z)$, $J_1(z)$ and $J_2(z)$ are the standard Bessel functions. The value $\tilde{a}$ is the ratio of the determinants of the monodromy matrices of the stable and the unstable PO. For $\tilde{a} \to 0$ one obtains the result of Ozorio de Almeida (Eq. (14)). The Maslov index is denoted by η and for the evaluation of g_E'' see, e.g., Ref. 57. A detailed description of these results can be found in Ref. 9.

To apply Eq. (15) small replacements are necessary: The action is given by $S = \hbar k l$, with k the wave number and l the length of the PO. The period of the PO can be expressed by its length and the term $M_2^3 g_E''$ be evaluated by using expressions from Ref. 9. Ullmo *et al.* have tested their trace formula numerically by applying it to a quartic oscillator for which they have calculated the first 12000 eigenvalues. They found good agreement between the simulated quantum spectrum and its reconstruction with Eq. (15). The two limiting cases, the Berry–Tabor result for integrable systems (Eq. (13)) and the Gutzwiller result for chaotic systems (Eq. (12)), are easily reproduced from Eq. (15). One obtains the first one for $\Delta S \to 0$, while the other results from the asymptotic expression for the Bessel functions.

For a test of the trace formula for near-integrable systems, Eq. (15), we studied experimentally a one-parameter family of superconducting two-dimensional microwave resonators. In Fig. 9 the shapes of the measured billiards are shown. They all belong to the family of Limaçon billiards, which have been numerically studied in Ref. 58. Their boundary is defined as the quadratic conformal mapping of the unit disc onto the complex

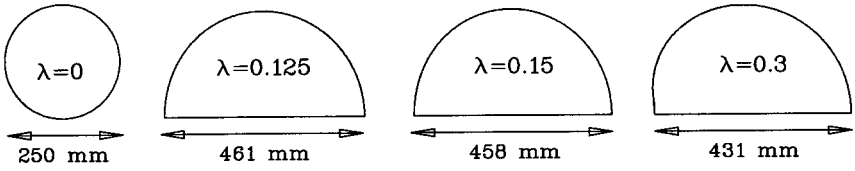

Fig. 9. Shapes of the investigated billiards of the Limaçon family. All billiards are desymmetrized, except the first one.

w-plane: $w = z + \lambda z^2$, where $\lambda \in [0, 1/2]$ controls the chaoticity of the system. In detail we have investigated four billiards of different chaoticity with parameters $\lambda = 0$, $\lambda = 0.125$, $\lambda = 0.15$ and $\lambda = 0.3$. All billiards, except the first one, are desymmetrized. For $\lambda = 0$ we have a circle, which is known to be integrable, i.e., regular. Investigations of the classical Poincaré surface of section of the other configurations have shown, that the fraction of the chaotic phase space is 55% ($\lambda = 0.125$), 66% ($\lambda = 0.15$) and nearly 100% ($\lambda = 0.3$), see Ref. 38.

The billiard cavities were excited with frequencies up to 20 GHz, so that a total number of more than 1000 resonances for each billiard (about 660 resonances for the circular billiard) has been detected. The high quality of the experimental spectra can be inferred from the example shown in Fig. 1 earlier. These eigenvalue sequences $\{k_1, k_2, ..., k_n\}$ form the basis for the following test of the trace formula (15) on the experimental side. Statistical studies of the microwave spectra have shown, that the quantum mechanical counterpart in terms of RMT of the classical Limaçon billiards exhibit the same degree of chaoticity so that these four billiards cover the full range from regular through mixed to chaotic dynamics.[38]

By applying the trace formula, Eq. (15), to the investigated systems, we restrict ourselves to the first periodic orbits up to a length of 1.4 m since then the length spectrum gets complicated due to interfering contributions from the so-called "whispering gallery" orbits (see Ref. 39 for details). The reconstruction of the spectrum of the circular billiard was done with the help of the Berry–Tabor formalism, one limiting case of Eq. (15), using a symbolic code which easily determines all periodic orbits.[59] For the three other billiards the properties of each PO (length, number of reflections, curvature of the boundary at the reflection point, Maslov index) were calculated numerically. The so found characteristic values for each PO form the basis for the reconstruction of the experimental spectra on the theoretical side.

A view at the square of the Fourier transformed fluctuating part of the spectral density of states is given in Fig. 10. Here a comparison between the experimental data and the numerical reconstruction for the four

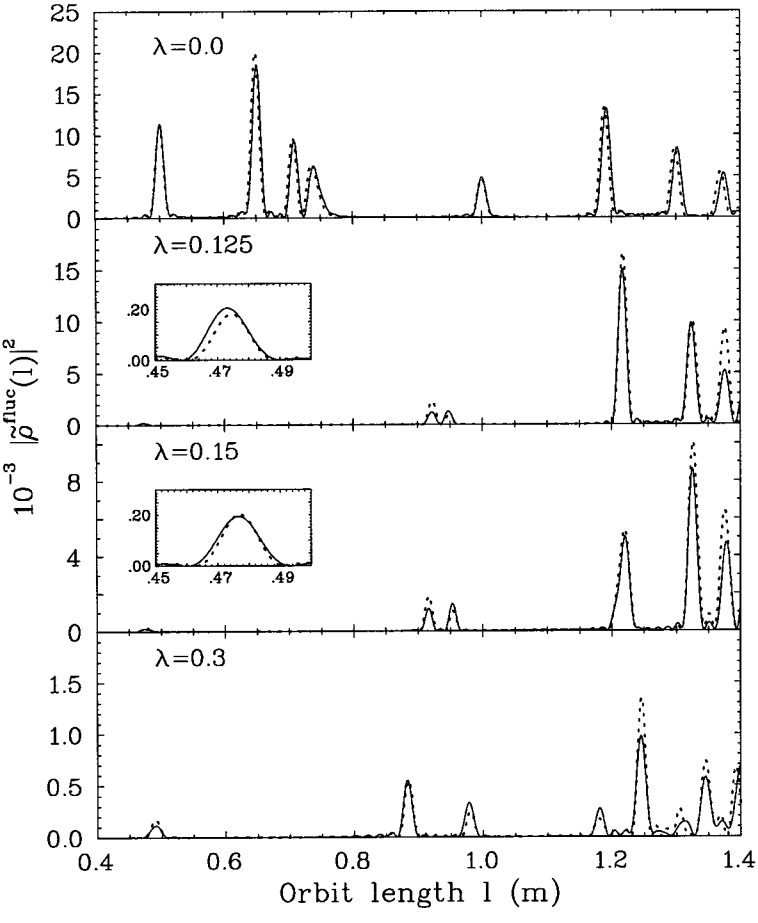

Fig. 10. Comparison between the measurement (solid line) and the reconstruction (dashed line) of length spectra with the help of the trace formula given by Eq. (15). The insets for the $\lambda = 0.125$ and $\lambda = 0.15$ billiard show a magnification of the first periodic orbit at $l \approx 0.47$ m (from Ref. 39).

investigated systems is presented. For the circle the reconstruction is in very good agreement with the measurement. The reconstruction for the two billiards belonging to the regime with mixed dynamics ($\lambda = 0.125$ and $\lambda = 0.15$ billiard) is for the shortest periodic orbits also in good agreement with the measured data, whereas for the following periodic orbits with length $l \geqslant 1.3$ m small deviations become visible. These deviations do not occur in the positions of the periodic orbits but in the height of the reconstructed peak. The same situation is found for the fully chaotic $\lambda = 0.3$

billiard, where the predictions of Gutzwiller's trace formula, Eq. (12), have been compared to the data.

The small deviations we found for the billiard systems with mixed dynamics ($\lambda = 0.125$ and 0.15) could be explained by two reasons: Equation (15) has been derived for the case of small perturbations of a regular system, i.e., the near-integrable case, while the two investigated billiards already constitute mixed systems. Furthermore the number of eigenvalues considered in the comparison (around 1000) are much smaller than Ullmo *et al.* have used for their numerical test (around 12000) with a quartic oscillator, so that we are probably still away from the semiclassical regime. Uncertainties of the experimental setup can be excluded for the deviations. Numerical simulations of the *ideal* system[42] show that the measured spectra agree very well with simulated ones, which allows a one-by-one comparison of the levels in the ideal and the real systems, respectively. The quantitative comparison shows that the measured sets of about 10^3 eigenfrequencies each are almost complete, with about 1 percent misinterpreted levels. Thus we can state that the data of the *real* system are accurate enough. Furthermore, as expected the results for the mixed systems obtained with the trace formula of Ullmo *et al.* is much more satisfying than using Gutzwiller's trace formula straightforwardly without taking the Poincaré–Birkhoff theorem into account. Finally, the small deviations found for the chaotic case ($\lambda = 0.3$) are indeed due to mechanical imperfections of the microwave cavity. In the manufacturing process the shaping of the boundary, in particular of the cusp at the lower left corner, caused some problems. Especially properties of the boundary, e.g., its curvature, determine the amplitude of the peak in the length spectrum.

5. THIRD EXAMPLE: THE THREE-DIMENSIONAL SINAI BILLIARD

Up to now, the semiclassical analysis of the measured spectra has been restricted to 2D-billiards; however, three-dimensional billiards are also of particular interest for realistic models of physical systems. Within the field of chaotic 3D-billiards the majority of experiments has been performed with electromagnetic (e.g., Refs. 27, 33, and 60) and acoustic (e.g., Ref. 32) waves, whereas the hardly feasible numerical modelling was restricted to very special geometries of high symmetry for the pure Schrödinger problem.[35]

Here we review briefly the results from an analysis[28] of the fully chaotic 3D-Sinai billiard respectively its desymmetrized version given by 1/48 of a cube with a sphere in its center, see Fig. 11. According to the experimental setup the system has to be described by the time-independent,

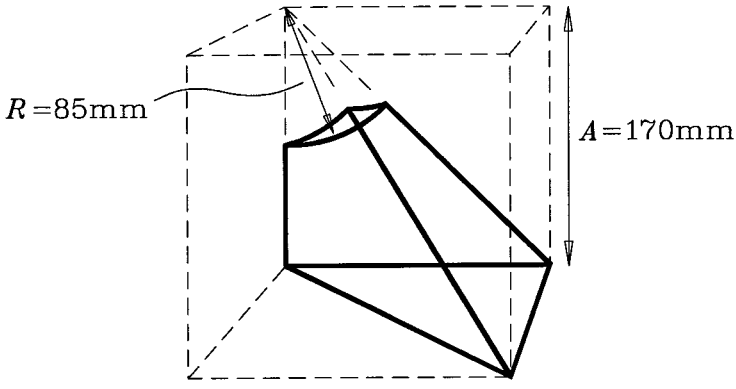

Fig. 11. Geometry of the desymmetrized 3D-Sinai billiard (boldface line) which constitutes one-sixth of the dashed cube. Eight of those cubes form the full system.

fully vectorial Helmholtz equation with electromagnetic boundary conditions ($\vec{E}_{||}|_{\partial\mathscr{G}} = \vec{0}$ and $\vec{B}_{\perp}|_{\partial\mathscr{G}} = \vec{0}$), see Eqs. (3)–(5). As the 2D-billiards discussed in this article, the electromagnetic resonator was also made of niobium and measured at 4.2 K. A detailed and accurate comparison of all measured spectra with different antenna combinations yielded a total set of approximately 1900 experimental resonances within the measured range. They formed the base of a statistical analysis in terms of RMT.

After rescaling the frequency axis to a mean level spacing of unity (as described in Sec. 3) we have examined the short-range correlations in the spectrum by calculating the nearest neighbor spacing distribution $P(s)$. As Fig. 12 shows the experimental data are very close to the GOE prediction for totally chaotic systems. Furthermore, we analyzed the spectrum on a larger scale in order to investigate long-range correlations. For this purpose we calculated $\Sigma^2(L)$, which expresses the variance of a number of resonances inside an interval of length L on the unfolded scale, as well as the related Dyson–Mehta statistics, $\Delta_3(L)$, also sensitive up to L, i.e., *several* mean level spacings. The result for both properties is given in Fig. 12 (l.h.s.). Here, two observations can be made: First, the experimental curves rapidly deviate from the GOE prediction and lie between the regular and the chaotic case. This behavior has also been observed in other experiments on three-dimensional systems.[32, 33] Second, above a certain value $L_{\max}$, which is different for both statistics ($L_{\max}^{\Sigma^2} \approx 40$, $L_{\max}^{\Delta_3} \approx 150$), the experimental curves run into saturation. This last feature—not seen in Refs. 32 and 33—is exactly what is expected from theory,[49] displaying the fact that for increasing L the given statistics is more and more sensitive to specific, i.e., non-universal features of the system.

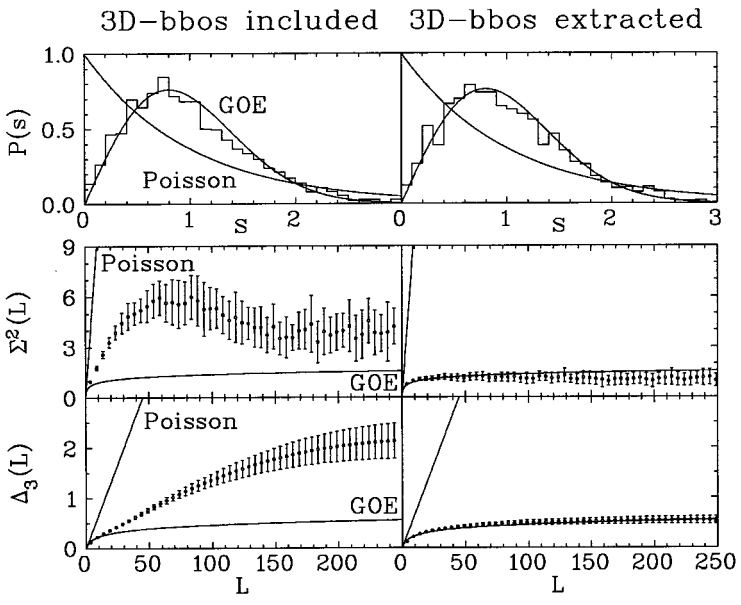

Fig. 12. Short- and long-range statistical measures before (left side) and after (right side) the extraction of fluctuations due to 3D-bouncing ball orbits. As can be seen, the strong deviation from the GOE curve is eliminated after the contribution of the bouncing ball orbits are extracted.[28]

Thus, although the system is fully ergodic on the classical side without any stable islands in phase space, the wave dynamical side pretends their existence. To understand this phenomenon, we analyzed the classical analogue in more detail. Therefore, we continued our investigation on a more specific scale which is a bridge between the classical chaotic features and their impact on the electromagnetic spectrum. This scale is given by the length spectrum of the billiard, which is obtained through the Fourier transform of the spectral level density. The resulting spectrum shows peaks at the classical periodic orbits of the billiard. Figure 13 exhibits the lower part of this spectrum up to a length $l = 1.5$ m. Here a rich structure of peaks can be observed above a minimum length $l_{\min} = 0.34$ m. The first peak belongs to the shortest 3D bouncing ball orbit (3D BBO) of the billiard, propagating along one edge of the desymmetrized cube without striking the sphere, see sketch in the inset.

As a matter of fact, the obtained length spectrum is totally dominated by BBOs of all possible dimensions, not only in the quantum case,[35] but also in the electromagnetic counterpart. To demonstrate this, we considered the contribution of the leading 3D BBOs to the given length spectrum.

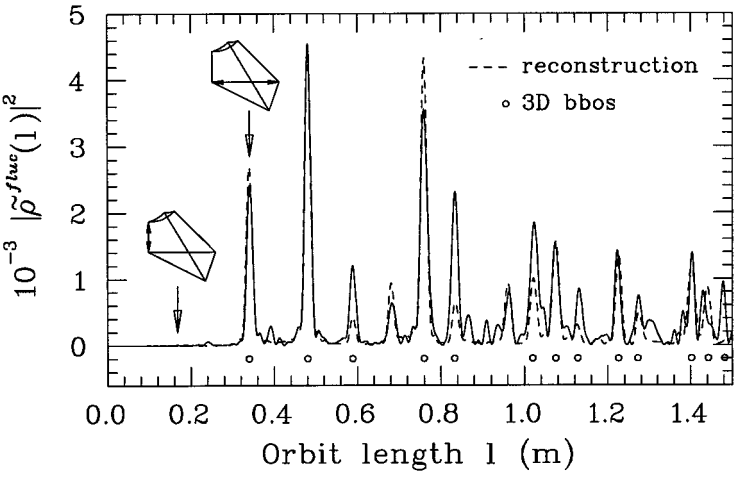

Fig. 13. Experimental length spectrum of the billiard (full line) and the semiclassical reconstruction using only 3D BBOs (dashed line). The picture in the inset show the first unstable and the first 3D BBO, respectively (from Ref. 28).

Therefore, we used a lattice vector description of Berry[61] to label and generate all 3D BBOs up to a certain length and determined their contribution through Eq. (10), but now adapted to the 3D-problem,[27]

$$N^{\mathrm{BBO}}(X)=\frac{2\pi S^{\mathrm{BBO}}}{l_{\mathrm{BBO}}^2}\left(\sum_{0<n<X}(X^2-n^2)-\frac{2}{3}X^3+\frac{1}{2}X^2\right) \tag{16}$$

with $X=l_{\mathrm{BBO}}f/c$. Here, the length of a given 3D BBO, l_{BBO}, was deduced directly from the lattice vector, and S^{BBO}, the perpendicular area on which this orbit exists, was fixed in a Monte-Carlo simulation. In the given range up to $l=1.5$ m, we obtained 55 3D BBOs of different degeneracies and with positive S^{BBO}; their superimposed semiclassical reconstruction due to Eq. (16) is given by the dashed line in Fig. 13. It is highly remarkable that nearly the full structure of the given length spectrum can be reproduced using only 3D BBOs, whereas the influence of the enormous number of unstable periodic orbits (approximately 36000 up to $l=1.5$ m) is hidden in the background. Discrepancies between the experimental length spectrum and the reconstruction can be predominantly found at the locations of the 3D BBOs themselves and arise because of the existence of the subdimensional and tangential BBO manifolds.[35]

To demonstrate the influence of the considered fluctuations due to 3D BBOs on the long-range measures Σ^2 and Δ_3, we repeated our statistical analysis using a modified unfolding procedure in which the contribution of

the 3D BBO is included. The result is given in Fig. 12 (r.h.s.) displaying, now also for Σ^2 and Δ_3, nearly perfect agreement with the GOE prediction in the universal regime up to $L_{\max}$, which is ≈ 75 for Σ^2. Therefore, saturation for Δ_3 is expected[62] at $L_{\max} \approx 300$.

For a proper reconstruction of the length spectrum with extracted BBO contribution of the here discussed electromagnetic case the trace formula of Gutzwiller is not applicable due to the polarization properties of the electromagnetic wave in the 3D-system. So, Balian and Duplantier[34] suggested a modified trace formula for this case, which takes these properties into account and reads as follows

$$\rho^{em}(S) \approx \mathrm{Re} \sum_{\mu,\ \mathrm{even}} 2 \cos \Psi_\mu A(S, \mathbf{M}_\mu) \exp\left(\frac{iS}{\hbar} - i\eta_\mu \frac{\pi}{2}\right) \tag{17}$$

It is very similar to $\rho^G(S)$ of Eq. (12),but the amplitude A has to be multiplied by a factor of $2 \cos \Psi_\mu$, which takes into account the rotation angle Ψ_μ of the polarization vector of a planar electromagnetic wave along the given unstable periodic orbit μ. Furthermore only orbits with an even number of reflections are considered in the leading order.

For an experimental test of this semiclassical description of electromagnetic problems the investigated 3D-Sinai billiard, however, is not a good candidate due to the large number of different BBOs which dominate the length spectrum. A 3D-stadium billiard,[63] see left side of Fig. 14, should show no (or only a few) BBOs. By reducing it to a quarter and with

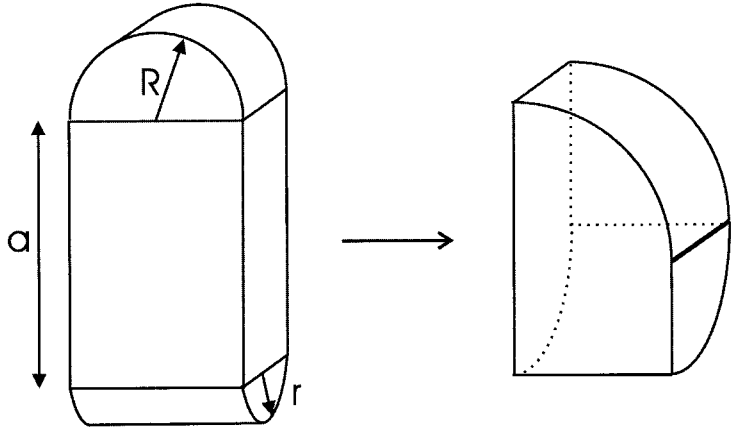

Fig. 14. Left side: full geometry of the 3D-stadium billiard. The quantities R and r are the radii of the two half-cylinders, respectively, and a is the distance between the two parts. Right side: desymmetrized version with vanishing length a.

a vanishing length a (right part of Fig. 14), only two BBO will survive and a test of the trace formula (Eq. (17)) by performing a microwave experiment should be possible, and we are in fact in the process of preparing such an experiment with a niobium cavity, whose dimensions are characterized by $R = 200$ mm and $r = 141$ mm.

6. CONCLUSION

Studying billiards modelled in form of microwave resonators is a powerful experimental technique for the investigations of quantum chaos and classical chaotic phenomena. For the particular subject of the present article –a test of trace formulas for spectra of billiards of varying degree of chaoticity –a prerequisite to this is a spectral resolution and a very good signal-to-noise ratio in the measured spectrum of eigenmodes, which can effectively be achieved by the use of superconducting microwave cavities. It is the quality of the spectra which assures the completeness of the obtained sequences of eigenvalues. Only then the statistical methods (RMT and POT) applied in the analysis to the data provide results of the necessary reliability. This becomes obvious in particular in the semiclassical analysis of Secs. 3 and 4 where the application of the trace formulas of Gutzwiller, Berry and Tabor and Ullmo, Grinberg and Tomsovic, to quantum spectra of billiards in the fully chaotic, regular and mixed regime, respectively, led to a theoretical reconstruction of the measured spectra. As pointed out in Sec. 5 it will certainly be a challenge to extend those investigations of trace formulas also to three-dimensional superconducting microwave billiards and are presently in the process of doing this.

ACKNOWLEDGEMENTS

It is a great pleasure for me to thank the collaborators in my group at Darmstadt, which consists at present of C. Dembowski, H.-D. Gräf, A. Heine, H. Rehfeld, and C. Richter, for their numerous contributions to the scientific material presented in this text and elsewhere in the literature. I am particular grateful to H. Rehfeld for his great effort in helping me to produce this manuscript. On the particular subject of trace formulas I have had very valuable advice in the past particularly from O. Bohigas, C. Lewenkopf, S. Tomsovic, D. Ullmo, H. A. Weidenmüller, A. Wirzba, and of course—especially at our time as Fellows at the Institute for Advanced Study Berlin during the Academic Year 1998/1999—from Martin Gutzwiller

to whom I dedicate this article with great pleasure and admiration for his seminal work in physics.

REFERENCES

1. M. C. Gutzwiller, *Chaos in Classical and Quantum Mechanics* (Springer, New York, 1990).
2. M. L. Mehta, *Random Matrices and the Statistical Theory of Energy Levels* (Academic Press, San Diego, 1991).
3. O. Bohigas, in *Chaos and Quantum Physics*, M.-J. Giannoni, A. Voros, and J. Zinn-Justin, eds. (Elsevier, Amsterdam, 1991), p. 87.
4. T. Guhr, A. Müller-Groeling, and H. A. Weidenmüller, *Phys. Rep.* **299**, 189 (1998).
5. M. C. Gutzwiller, *J. Math. Phys.* **12**, 343 (1971).
6. A. Einstein, *Verhandl. Deutsch. Physikal. Ges.* **19**, 82 (1917). L. Brillouin, *J. Phys. Rad.* **7**, 353 (1926). J.B. Keller, *Ann. Phys. (N.Y.)* **4**, 180 (1958).
7. M. C. Gutzwiller, *J. Math. Phys.* **11**, 1792 (1970).
8. M. V. Berry and M. Tabor, *Proc. R. Soc. Lond. A* **349**, 101 (1976). M. V. Berry and M. Tabor, *J. Phys. A* **10**, 371 (1977).
9. D. Ullmo, M. Grinberg, and S. Tomsovic, *Phys. Rev. E* **54**, 136 (1996). S. Tomsovic, M. Grinberg, and D. Ullmo, *Phys. Rev. Lett.* **75**, 4346 (1995).
10. G. D. Birkhoff, *Acta. Math.* **50**, 359 (1927).
11. Ya. G. Sinai, *Sov. Math. Dokl.* **4**, 1818 (1963).
12. L. A. Bunimovich, *Zh. Éksp. Teor. Fiz.* **89**, 1452 (1985) [*Sov. Phys. JETP* **62**, 842 (1985)].
13. P. Sarnak, *Israel Math. Conf. Proc.* **8**, 183 (1995).
14. S. W. McDonald and A. N. Kaufman, *Phys. Rev. Lett.* **42**, 1189 (1979).
15. F. Steiner, in *Schlaglichter der Forschung, Zum 75. Jahrestag der Universität Hamburg 1994*, R. Ansorge, ed. (Reimer, Berlin, 1994), p. 543.
16. M. V. Berry, *Proc. R. Soc. Lond. A* **413**, 183 (1987).
17. H.-J. Stöckmann and J. Stein, *Phys. Rev. Lett.* **64**, 2215 (1990).
18. S. Sridhar, *Phys. Rev. Lett.* **67**, 785 (1991).
19. J. Stein and H.-J. Stöckmann, *Phys. Rev. Lett.* **68**, 2867 (1992).
20. H.-D. Gräf, H. L. Harney, H. Lengeler, C. H. Lewenkopf, C. Rangacharyulu, A. Richter, P. Schardt, and H. A. Weidenmüller, *Phys. Rev. Lett.* **69**, 1296 (1992).
21. P. So, S. M. Anlage, E. Ott, and R. N. Oerter, *Phys. Rev. Lett.* **74**, 2662 (1995).
22. H.-J. Stöckmann, *Quantum Chaos: An Introduction* (Cambridge University Press, Cambridge, 1999).
23. H. Alt, C. Dembowski, H.-D. Gräf, R. Hofferbert, H. Rehfeld, A. Richter, and C. Schmit, *Phys. Rev. E* **60**, 2851 (1999).
24. H. Alt, H.-D. Gräf, H. L. Harney, R. Hofferbert, H. Lengeler, C. Rangacharyulu, A. Richter, and P. Schardt, *Phys. Rev. E* **50**, 1 (1994).
25. H. Alt, H.-D. Gräf, H. L. Harney, R. Hofferbert, H. Lengeler, A. Richter, P. Schardt, and H. A. Weidenmüller, *Phys. Rev. Lett.* **74**, 62 (1995).
26. H. Alt, C. I. Barbosa, H.-D. Gräf, T. Guhr, H. L. Harney, R. Hofferbert, H. Rehfeld, and A. Richter, *Phys. Rev. Lett.* **81**, 4847 (1998).
27. H. Alt, H.-D. Gräf, R. Hofferbert, C. Rangacharyulu, H. Rehfeld, A. Richter, P. Schardt, and A. Wirzba, *Phys. Rev. E* **54**, 2303 (1996).
28. H. Alt, C. Dembowski, H.-D. Gräf, R. Hofferbert, H. Rehfeld, A. Richter, R. Schuhmann, and T. Weiland, *Phys. Rev. Lett.* **79**, 1026 (1997).
29. J. D. Jackson, *Classical Electrodynamics*, 2nd edn. (Wiley, New York, 1975).

30. M. R. Schroeder, *J. Audio Eng. Soc.* **35**, 307 (1987), originally published in *Acustica* **4**, 456 (1954).
31. R. L. Weaver, *J. Acoust. Soc. Am.* **85**, 1001 (1989).
32. C. Ellegaard, T. Guhr, K. Lindemann, H. Q. Lorensen, J. Nygård, and M. Oxborrow, *Phys. Rev. Lett.* **75**, 1546 (1995). P. Bertelsen, C. Ellegaard, T. Guhr, M. Oxborrow, and K. Schaadt, *Phys. Rev. Lett.* **83**, 2171 (1999).
33. S. Deus, P. M. Koch, and L. Sirko, *Phys. Rev. E* **52**, 1146 (1995).
34. R. Balian and B. Duplantier, *Ann. Phys. (N.Y.)* **104**, 300 (1977).
35. H. Primack and U. Smilansky, *Phys. Rev. Lett.* **74**, 4831 (1995).
36. O. Frank and B. Eckhardt, *Phys. Rev. E* **53**, 4166 (1996).
37. M. Henseler, A. Wirzba, and T. Guhr, *Ann. Phys. (N.Y.)* **258**, 286 (1997).
38. A. Richter, in *Emerging Applications of Number Theory* (The IMA Volumes in Mathematics and Its Applications, Vol. 109), D. A. Hejhal, J. Friedman, M. C. Gutzwiller, and A. M. Odlyzko, eds. (Springer, New York, 1999), p. 479.
39. C. Dembowski, H.-D. Gräf, A. Heine, T. Hesse, H. Rehfeld, and A. Richter, *Phys. Rev. Lett.*, submitted.
40. A. Richter, in *Proc. 5th European Particle Accelerator Conference*, S. Meyers *et al.*, eds. (IOP Publishing, Bristol and Philadelphia, 1996), p. 110.
41. C. Dembowski, H.-D. Gräf, A. Heine, R. Hofferbert, H. Rehfeld, and A. Richter, *Phys. Rev. Lett.* **84**, 867 (2000).
42. T. Hesse, Dissertation, University of Ulm, Germany, 1997.
43. E. B. Bogomolny, *Physica D* **31**, 169 (1988).
44. H. Weyl, *J. Reine Angew. Math.* **141**, 1 (1912); ibid. 163; *J. Reine Angew. Math.* **143**, 177 (1913).
45. H. P. Baltes and E. R. Hilf, *Spectra of Finite Systems* (Bibliographisches Institut, Mannheim, 1975).
46. T. A. Brody, J. Flores, J. B. French, P. A. Mello, A. Pandey, and S. S. M. Wong, *Rev. Mod. Phys.* **53**, 419 (1981).
47. M. V. Berry and M. Robnik, *J. Phys. A* **17**, 2413 (1984).
48. M. Sieber, U. Smilansky, S. C. Creagh, and R. G. Littlejohn, *J. Phys. A* **26**, 6217 (1993).
49. M. V. Berry, *Proc. R. Soc. Lond. A* **400**, 229 (1985).
50. M. Sieber and F. Steiner, *Physica A* **44**, 248 (1990).
51. D. Alonso and P. Gaspard, *J. Phys. A* **27**, 1599 (1994).
52. J. Stein and H.-J. Stöckmann, *Phys. Rev. Lett* **68**, 2867 (1992).
53. A. Dürer, *Underweysung der Messung mit dem Zirckel un Richtscheyt in Linien, Ebnen und Ganzten Corporen*, 2nd edn. (Uhl, Nördlinegn, 1983).
54. M. V. Berry, *Eur. J. Phys.* **2**, 91 (1981).
55. A. Bäcker, F. Steiner, and P. Stifter, *Phys. Rev. E* **52**, 2463 (1995).
56. A. M. Ozorio de Almeida, *Hamiltonian Systems: Chaos and Quantization* (Cambridge University Press, Cambridge, 1988).
57. O. Bohigas, S. Tomsovic, and D. Ullmo, *Phys. Rep.* **223**, 43 (1993).
58. M. Robnik, *J. Phys. A* **16**, 3971 (1983); *J. Phys. A* **17**, 1049 (1984).
59. R. Balian and B. Bloch, *Ann. Phys.* **64**, 76 (1971).
60. U. Dörr, H.-J. Stöckmann, M. Barth, and U. Kuhl, *Phys. Rev. Lett.* **80**, 1030 (1998).
61. M. V. Berry, *Ann. Phys.* **131**, 163 (1981).
62. A. Delon, R. Jost, and M. Lombardi, *J. Chem. Phys.* **95**, 5701 (1991).
63. T. Papenbrock, *Phys. Rev. E* **61**, 4626 (2000).